Geoid
Journal of Geodesy and Geomatics

Geoid Vol. 21, No. 1, 2026, 47-63

P-ISSN: 1858-2281; E-ISSN: 2442-3998

Identification of the Best Semivariogram Model for the Blending of In-Situ and ERA5-Land Air Temperature Data Using the Kriging with External Drift Technique

Fatchiyah[*1,2], Eko Yuli Handoko[1], Ardhasena Sopaheluwakan[2], Robi Muharsyah[2]
[1]Department of Geomatics Engineering, Institut Teknologi Sepuluh Nopember, 60111, Surabaya, Indonesia
[2]Agency for Meteorology Climatology and Geophysics (BMKG), 10610, Jakarta, Indonesia
*Corresponding author: fati.fatchiyah@gmail.com

Received: 21 November 2025; Revised: 10 December 2025; Accepted: 16 December 2025; Published: 6 January 2026

Abstract: Accurate air temperature monitoring is essential for understanding climate dynamics and microclimates, particularly in regions with diverse topography. The limited number of observation stations often results in data that do not fully represent actual conditions. To address this gap, combining in-situ measurements with ERA5-Land reanalysis presents a promising alternative, although ERA5-Land may still exhibit biases in mountainous or urban areas. This study applies Kriging with External Drift (KED) to improve temperature estimation, focusing on identifying the most suitable semivariogram model. Daily and monthly analyses were conducted, with performance evaluated using RMSE, MAE, and MSE. The results indicate that the Spherical model consistently performs best for average and maximum temperatures, while the Exponential model provides better estimates for minimum temperature at the daily scale, and the Linear model at the monthly scale. These findings demonstrate that KED can significantly enhance temperature estimation in areas with sparse observations, while also highlighting the most reliable semivariogram models for different temperature parameters.

Keywords : Air temperature, ERA5-Land, KED, Semivariogram

How to cite: Fatchiyah., Handoko, E.Y., Syariz, M.A & Sopaheluwakan, A. (2025). Identification of the Best Semivariogram Model for the Blending of In-Situ and ERA5-Land Air Temperature Data using the Kriging With External Drift Technique. *Geoid 21*(1), 47-63.

Introduction

Air temperature, as a key indicator of thermal energy distribution in the atmosphere, has far-reaching implications across various sectors, including ecosystems, agriculture, public health, and the economy (Carleton & Hsiang, 2016; Abbass et al., 2022). Several factors, such as solar radiation, humidity, atmospheric pressure, and geographic conditions, influence air temperature (Shamshiri et al., 2018; Zhao et al., 2021; Ainurrohmah & Sudarti, 2022). Accurate temperature monitoring is vital not only for short-term weather predictions but also for supporting the development of climate change mitigation policies and adaptation strategies based on empirical data (Abbas et al., 2022).

A major challenge in achieving accurate air temperature measurements arises from the limited number of in-situ observation stations and the geographical complexity of regions such as East Java. This area, with its diverse climatic conditions linked to varied topography—from coastal zones to mountainous regions—creates significant microclimatic variability. This variability presents a challenge for obtaining reliable temperature data due to the sparse distribution of observation stations (Hidayati & Suryanto, 2015). Furthermore, this limitation hampers the comprehensive understanding of micro- and regional climate change (Aldrian et al., 2011). Although expanding the network of observation stations is necessary, this expansion is constrained by high costs and logistical challenges.

Currently, ERA5-Land data from the European Centre for Medium-Range Weather Forecasts (ECMWF) offers spatial temperature data with relatively high resolution (Hersbach et al., 2020; Muñoz-Sabater et al., 2021). ERA5-Land employs data assimilation techniques, integrating various satellite datasets to provide optimal climate observations with a spatial resolution of up to 9 km (Muñoz-Sabater et al., 2021; C3S, 2022). However, the accuracy of ERA5-Land temperature estimates is limited, particularly in areas with

complex topographies, such as mountainous or urban regions, where biases and inaccuracies are more prevalent (Zhao & He, 2022).

To address the challenge of improving temperature estimation, a promising approach involves combining limited in-situ data with high-resolution spatial observation data. One such technique, Kriging with External Drift (KED), uses spatial information as a 'drift' to enhance the accuracy of temperature estimations at specific locations (Hudson & Wackernagel, 1994). The KED method involves constructing a variogram and semivariogram to identify the spatial model that best fits the characteristics of the available data (Oliver & Webster, 2014). While the variogram captures the relationship between observation points, the semivariogram describes the spatial correlation of temperature differences between two points, taking distance and orientation into account (Bohling, 2005).

Previous research on KED has primarily focused on selecting the appropriate 'drift' data, with less attention given to the choice of semivariogram model. The correct selection of a semivariogram model is crucial for ensuring accurate interpolation, especially in regions with significant topographical variations (Ly et al., 2011). Therefore, this study aims to identify the optimal semivariogram model for KED and assess its performance in improving temperature estimation accuracy by integrating ERA5-Land as the 'drift'. It is anticipated that the findings of this research will contribute to overcoming the challenge of insufficient air temperature observation density in areas lacking in-situ stations, ultimately providing more accurate temperature data for those regions.

Data and Methods

This study was conducted in East Java Province, located between 111°00' E – 114°04' E and 7°12' S – 8°48' S. The region encompasses coastal lowlands along the coastline and volcanic mountainous areas, resulting in significant elevation variations (Figure 1). This topographical diversity leads to pronounced differences in meteorological parameters, with a primary focus on air temperature. The research utilized daily air temperature data (°C), specifically maximum (Tmax), average (Tave), and minimum (Tmin) temperatures, spanning from 2019 to 2023 (5 years), collected from 10 BMKG observation stations (Table 1). The data were sourced from BMKGSoft, a software application developed by the Indonesian Meteorological, Climatological, and Geophysical Agency (BMKG) for storing and providing observational data. The dataset used in this study was prioritized for completeness (above 90%) and had undergone a thorough quality control process to ensure data accuracy.

In addition to the in-situ data from BMKG stations, the study also incorporated reanalysis air temperature data from the ECMWF's ERA5-Land, which provides spatial resolution of approximately 9 km and daily temporal resolution (Muñoz-Sabater et al., 2021). ERA5-Land data, covering the period from 1950 to the present, are freely accessible via the ECMWF website (Copernicus Climate Change Service, 2022). Differences in the spatial and temporal resolutions between in-situ air temperature observations (point-based data) and ERA5-Land data (grid-based) were addressed through a harmonization process prior to blending the datasets using Kriging with External Drift (KED). From a spatial perspective, the ERA5-Land data, which are provided on a 0.1° × 0.1° grid, were projected onto the locations of BMKG stations by extracting the nearest grid-cell value or applying nearest-neighbor interpolation. These approaches are commonly used to reconcile the spatial support between gridded and point-based datasets (Li & Heap, 2014). This procedure ensures that each station is assigned an ERA5-Land value that is spatially representative of its location, allowing both datasets to share a consistent spatial basis and to be reliably integrated into subsequent geostatistical modelling.

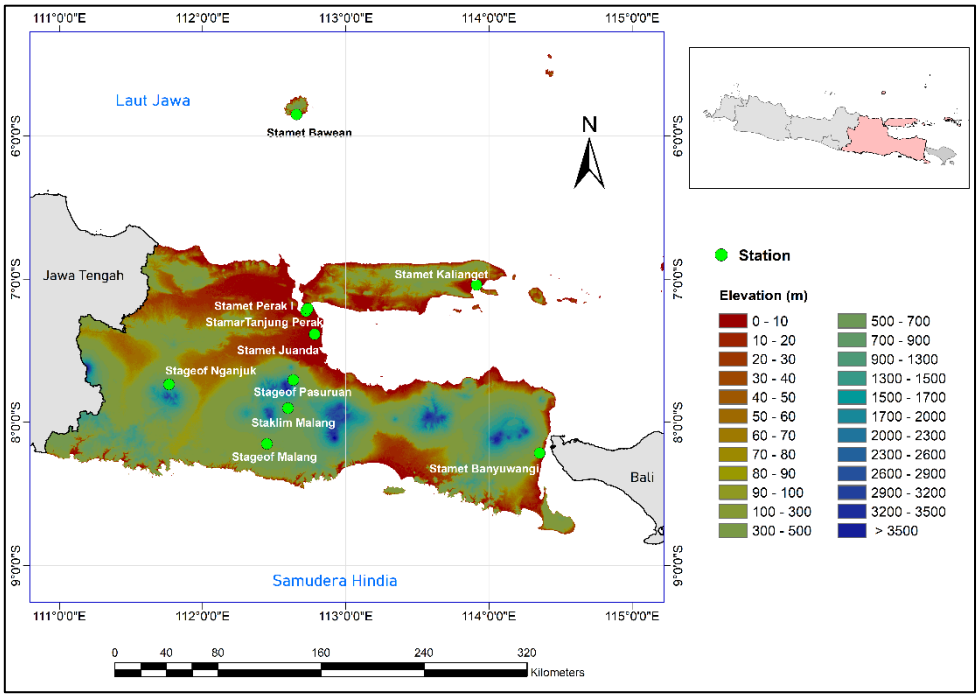

Figure 1. Map of the study area.

Table.1. BMKG Observation Stations in East Java

No.	Station Name	Latitude	Longitude	Elevation (m)
1	Stasiun Meteorologi Sangkapura	-5.85	112.66	3
2	Stasiun Meteorologi Perak I	-7.22	112.72	3
3	Stasiun Meteorologi Juanda	-7.38	112.78	3
4	Stasiun Meteorologi Maritim Tanjung Perak	-7.21	112.74	3
5	Stasiun Klimatologi Malang	-7.90	112.60	590
6	Stasiun Geofisika Pasuruan	-7.70	112.64	832
7	Stasiun Geofisika Malang	-8.15	112.45	285
8	Stasiun Meteorologi Kalianget	-7.04	113.91	3
9	Stasiun Geofisika Nganjuk	-7.73	111.77	723
10	Stasiun Meteorologi Banyuwangi	-8.22	114.36	52

From a temporal perspective, the hourly ERA5-Land data were converted to daily resolution to match the temporal scale of the station observations. This aggregation was performed by calculating the daily minimum, maximum, or mean temperature from the 24 hourly values, following standard procedures for converting reanalysis data to daily metrics (Tarek et al., 2020). Through this process, the two datasets achieve temporal equivalence and can be paired according to the same observation dates. The results of this spatio-temporal harmonization are subsequently incorporated into the Kriging with External Drift (KED) framework, where the extracted ERA5-Land values serve as the external drift variable that captures large-scale temperature patterns, while the in-situ BMKG observations provide the local-scale residual information. The KED approach is both theoretically and empirically designed to merge broad-scale predictors with point-based local

observations, thereby producing higher-resolution estimates with markedly improved accuracy (Hengl et al., 2007; Hengl et al., 2018). Furthermore, the use of ERA5-Land as the drift predictor is strongly supported by the stable, spatially coherent, and physically consistent characteristics of the reanalysis product (Hersbach et al., 2020). Consequently, the initial differences in spatial and temporal resolution between the two datasets are not merely resolved but are strategically exploited through geostatistical integration to enhance the precision and reliability of the high-resolution temperature estimates.

Kriging with External Drift (KED)

As summarized by Varentsov et al. (2020), Kriging with External Drift (KED) is a geostatistical technique designed to improve the accuracy of spatial data interpolation by integrating in-situ observations with external data, referred to as a 'drift,' which influences the variable under analysis, such as air temperature. The external data serves as an additional predictor to capture spatial variability that may not be represented by in-situ measurements.

Mathematically, the KED estimation can be expressed as follows:

$$\hat{z}(s_0) = m(s_0) + \sum_{i=1}^{n} \lambda_i \left(z(s_i) - m(s_i)\right) \quad (1)$$

Where:

$\hat{z}(s_0)$ = the estimated value at the target location,
$m(s_o)$ = the deterministic estimate at location s_o based on the external or drift model (ERA5-Land)
λ_i = the Kriging weight calculated based on the spatial variogram between the target location s_o and the measurement point s_i,
$\hat{z}(s_i)$ = the measured value at the point s_i ,
$m(s_i)$ = the external drift value at the point s_i

A fundamental component of KED is the semivariogram, which describes the spatial relationship between the in-situ temperature data and the ERA5-Land temperature data used as the drift. It estimates the spatial dependence pattern between the two datasets (Mazzella & Mazzella, 2013; Oliver & Webster, 2015).

The Semivariogram is formulated as follows:

$$\gamma(h) = \frac{1}{2}\sum [Z(s) - Z(s+h)]^2 \quad (2)$$

The semivariogram is defined by three primary parameters: nugget, sill, and range, as depicted in Figure 2. The nugget represents the semivariogram value at zero distance on the vertical axis and indicates variability at a very small scale, such as local fluctuations or measurement errors (Tang et al., 2021). The sill denotes the maximum value the semivariogram reaches after the range, illustrating the degree to which data variability can be explained by the spatial structure. The range is the distance at which the semivariogram levels off, signaling that data points beyond this distance no longer exhibit significant spatial correlation. These parameters are crucial in determining the accuracy of the KED model when predicting values at unobserved locations (Goovaerts, 1997; Chen et al., 2019). In this study, the semivariogram model was computed using the Python module pykrige (Murphy et al., 2024), which automates the estimation of the sill, nugget, and range parameters.

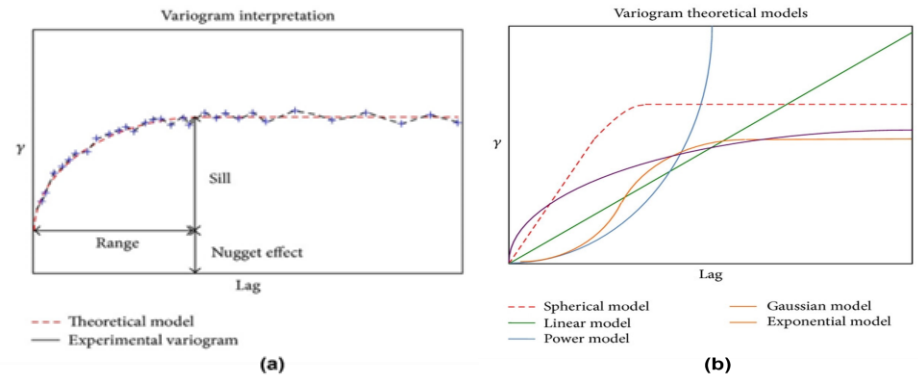

Figure 2. (a) Semivariogram Plot, (b) Theoretical Semivariogram Model Plot (Mazzella, A., and Mazzella, A., 2013)

The study examined five semivariogram models: Spherical, Exponential, Power, Linear, and Gaussian. Each of these models has distinct advantages and limitations, which form the primary focus of this research. A summary of the specific formulations for each semivariogram model is presented in Table 2.

Table 2. Semivariogram Model Calculation Formulas

Semivariogram Models	**Equation**
Spherical	$\gamma(h) = \begin{cases} C_0 + C\left[\left(\frac{3h}{2a}\right) - 0.5\left(\frac{h}{a}\right)^3\right] & \text{for } h \le a \\ C_0 + C & \text{for } h > a \end{cases}$
Exponential	$\gamma(h) = C_0 + C\left[1 - \exp\left(-\frac{3h}{a}\right)\right]$
Gaussian	$\gamma(h) = C_0 + C\left[1 - \exp\left(-\frac{-3h^2}{a^2}\right)\right]$
Linear	$\gamma(h) = \begin{cases} C_0 + C_1 . h, & \text{for } 0 \le h \le h_0 \\ C_0 + C_1 . h_0, & \text{for } h > h_0 \end{cases}$
Power	$\gamma(h) = C_0 + Ch^p$

where:

$\gamma(h)$ = Semivariance at lag distance
h = Lag distance between data points,
C_0 = Nugget effect, which is the semivariance at a very small distance (h=0),
C = The partial sill, which is the maximum value of the semivariance (excluding the nugget effect),
$C_0 + C$ = Sill (Total Sill), the value of the semivariogram when the distance is large and the semivariance becomes constant
A = Range, the distance at which the semivariance reaches the sill.

Cross-Validation Technique

To assess the reliability of the temperature predictions generated by the KED method, cross-validation is employed as the first step. This resampling technique is widely used for selecting and evaluating the performance of predictive models (Berrar, 2019). A commonly applied cross-validation approach is Leave-One-Out Cross-Validation (LOOCV), which is particularly effective for evaluating predictive performance in

spatial data (Berrar, 2019). In this study, LOOCV was used to assess the performance of each semivariogram model within the KED framework, utilizing data from all 10 observation stations (10 locations × 1825 days, or 5 years).

For each iteration on day t, one station is excluded from the dataset to serve as the validation point, while the remaining nine stations are used to construct the semivariogram model to estimate the temperature for the excluded station on day t. This process is repeated by rotating the validation station in each iteration (Figure 3). At the end of the process, a dataset of estimated temperatures for all 10 station locations is generated for each semivariogram model. This dataset is then analyzed to evaluate the performance of each semivariogram model.

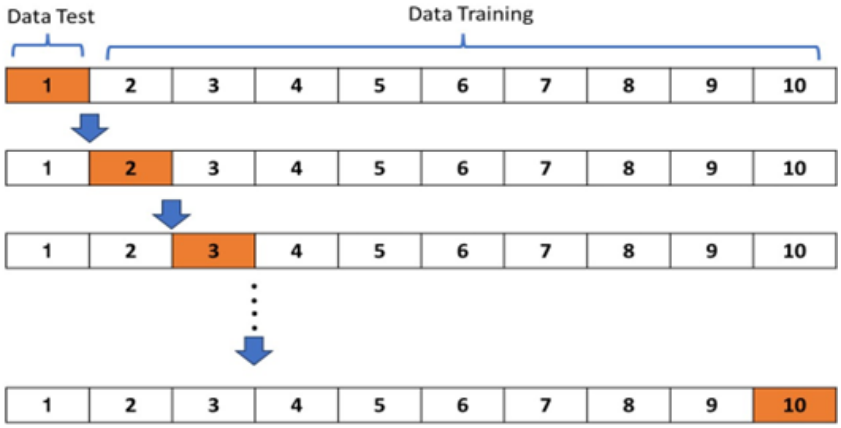

Figure 3. LOOCV (Leave-One-Out-Cross-Validation) process

Statistical Evaluation Metrics

The selection of an appropriate semivariogram model for the Kriging with External Drift (KED) technique is essential for ensuring the accuracy of temperature estimation results. In this study, the performance of the KED semivariogram models is assessed by evaluating the error levels using three metrics: Root Mean Squared Error (RMSE), Mean Absolute Error (MAE), and Mean Squared Error (MSE) (Hodson, 2022).

These metrics are employed to determine how closely the model's predictions align with the actual values. RMSE calculates the square root of the mean of the squared differences between predicted and observed values, with lower values indicating better model performance. MAE measures the average of the absolute differences between predicted and observed values, offering insights into the model's stability. On the other hand, MSE computes the mean of the squared deviations between predictions and actual observations, making it more sensitive to outliers, where lower values signify more accurate estimations. The formulas for each of these metrics are presented in Table 3.

Table 3. Metric Calculation Formula

Metrics	Equation	Range (Perfect)
RMSE *(Root Mean Squared Error)*	$\sqrt{\frac{1}{n}\sum_{i=1}^{n}(y_i - \hat{y}_i)^2}$	0 to ∞
MAE *(Mean Absolute Error)*	$\frac{1}{n}\sum_{i=1}^{n}\lvert y_i - \hat{y}_i\rvert$	0 to ∞

MSE *(Mean Squared Error)*	$\frac{1}{n}\sum_{i=1}^{n}(y_i - \hat{y}_i)^2$	0 to ∞

Where:

y_i = observation value

$\hat{y}_i$ = predicted value

n = number of data

$\bar{y}$ = average value of observations

Results And Discussion

Comparison of In-situ Observation Temperature Data and ERA5-Land

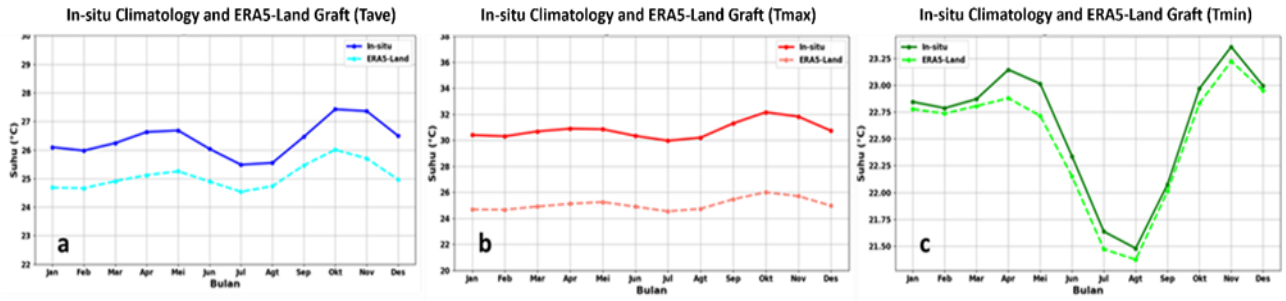

Figure 4. Climatological comparison between in-situ observation temperature values and ERA5-Land at three types of temperature, Tave (a), Tmax (b), Tmin (c) for all stations in East Java

Figure 4 illustrates a comparison of the climatological values for three types of temperature: average temperature (Tave) (a), maximum temperature (Tmax) (b), and minimum temperature (Tmin) (c), between in-situ observation data and ERA5-Land data, averaged across all stations in East Java. Visually, significant differences between the two datasets are observed, with the exception of Tmin. Overall, the in-situ data tend to show higher temperature values compared to ERA5-Land across all temperature types, particularly for Tave and Tmax. While ERA5-Land generally provides lower temperature estimates, it accurately captures the climatological patterns of all three temperature types, especially in representing Tmin. This suggests that although ERA5-Land data tend to underestimate the actual air temperature in East Java, they still provide a reasonable approximation of temperature trends.

To further explore the relationship between temperature and elevation, Figure 5 presents a comparison of the three temperature types at two selected stations representing distinct locations: the lowland Tanjung Perak Station (Figure 5a, 5b, and 5c) and the highland Malang Geophysics Station (Figure 5d, 5e, and 5f). At the daily temporal scale, both datasets exhibit similar overall temperature patterns at both stations. While a bias between ERA5-Land and in-situ data is apparent, the temperature trends (increases and decreases) over the observation period show that ERA5-Land values closely align with in-situ observations at specific times, particularly for Tmin. However, for Tave and Tmax, a noticeable bias exists between the two datasets. These findings indicate that while ERA5-Land temperature estimates generally follow the observed temperature patterns, they exhibit discrepancies, particularly for higher temperatures, across stations with varying elevations.

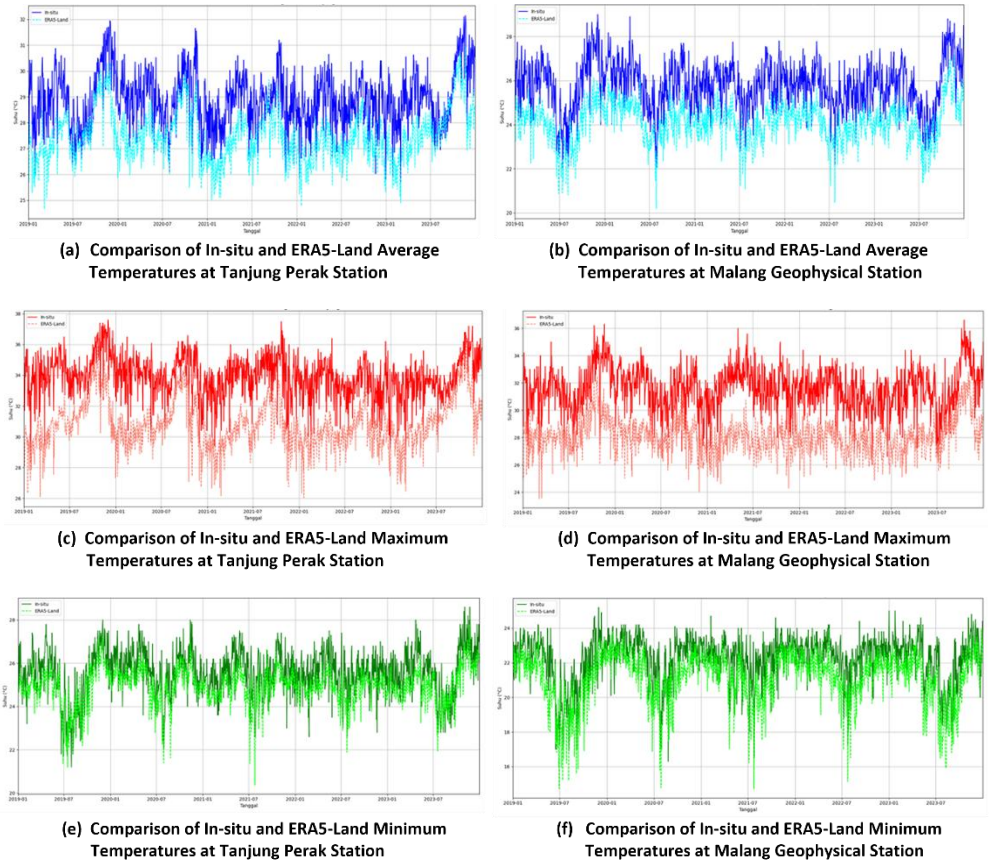

Figure 5. Comparison between in-situ and ERA5-Land temperature values for Tave, Tmax, Tmin at Tanjung Perak Station (a,c,e) and Malang Geophysical Station (b,d,f)

Temperature Correlation Between Observation Locations

Prior to evaluating the performance of Kriging with External Drift (KED), it is crucial to examine the relationship and temperature patterns across the stations in East Java. This spatial correlation analysis serves as an essential foundation for integrating in-situ and ERA5-Land data, as it quantifies the degree of similarity in the temporal temperature patterns between different locations.

The correlation results (Figure 6) generally align with the fundamental geographical principle that the closer the distance between stations, the higher the correlation. A strong correlation suggests that stations share similar environmental conditions, while a weaker correlation indicates significant temperature variations due to local geographical features and microclimatic influences (Yang et al., 2018; Chen et al., 2021). A clear example of this is the correlation between Tanjung Perak and Perak I stations, which are located approximately 2 km apart and exhibit an almost perfect correlation (0.94). This high correlation likely reflects the influence of homogeneous factors such as proximity to the sea or the urban heat island effect (Zhou et al., 2020).

In contrast, larger distances and topographical variations lead to weaker temperature correlations. For instance, Banyuwangi Station, situated at the eastern edge of East Java, shows a significantly lower correlation (0.38) with Sangkapura Station, due to the considerable geographical separation. Elevation differences also influence correlations; for example, the Malang Geophysics Station (285 meters above sea level) exhibits a moderate correlation (0.65) with Pasuruan Geophysics Station, which is at a similar elevation, highlighting the impact of the lapse rate and mountainous climate. This correlation analysis provides valuable insights for modeling the spatial temperature structure in the KED framework.

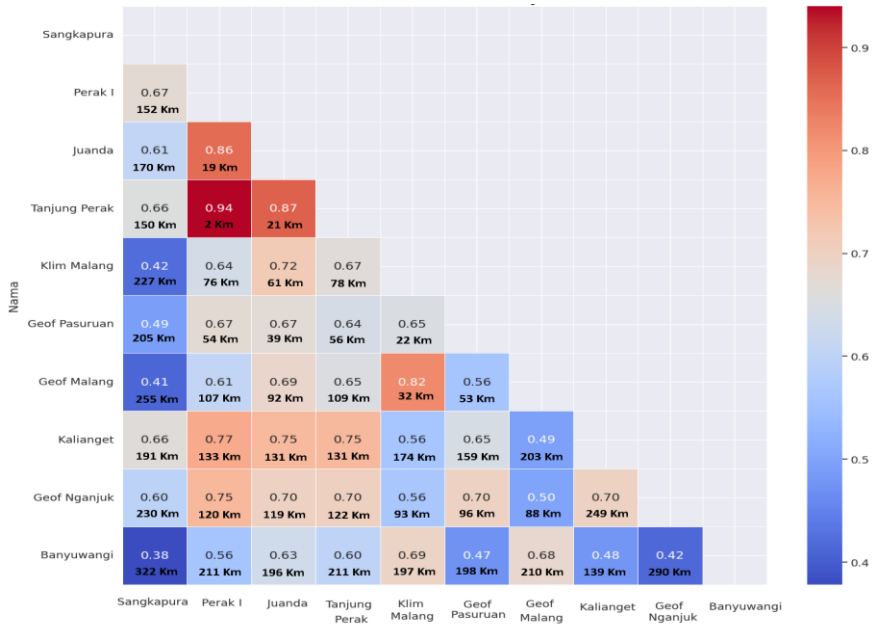

Figure 6. Correlation Matrix of Tave Between Observation Locations in East Java

Semivariogram Model Selection

Prior to conducting temperature estimation using Kriging with External Drift (KED), the selection of an appropriate semivariogram model is performed. This step is critical as it directly influences the accuracy of the KED estimation. The semivariogram model is selected based on KED's ability to predict temperature at two temporal scales: daily and monthly, across all stations in East Java. The parameters of the sill, nugget, and range are automatically determined using the PyKrig function in Python, with a binning configuration of 20 bins. The semivariogram models are evaluated for three types of temperature: average temperature (Tave), maximum temperature (Tmax), and minimum temperature (Tmin), utilizing five different semivariogram models: Exponential, Gaussian, Linear, Power, and Spherical. Each model is assessed based on three error metrics Root Mean Square Error (RMSE), Mean Absolute Error (MAE), and Mean Squared Error (MSE) to evaluate its precision and stability in estimating in-situ observed temperature values.

Evaluation at the Daily Scale

At the daily scale, the performance of each KED semivariogram model exhibits distinct patterns, as depicted in Figure 7. The Exponential, Spherical, and Gaussian models display similar values for the sill, nugget, and range. Specifically, the Exponential model shows a relatively large nugget, a moderate range, and quickly reaches the sill; the Spherical model demonstrates a small nugget, a clear range, and a stable approach to reaching the sill; and the Gaussian model presents a small nugget with a more extended range. In contrast, the Power and Linear models tend to show irregular patterns, with unclear or absent values for the nugget, sill, and range.

Based on the analysis of the daily data, the Spherical model exhibits the best performance for predicting average temperature (Tave), with RMSE = 1.042, MAE = 0.789, and MSE = 1.085, which are lower than those of the other models. This suggests that the Spherical model is more effective in minimizing errors in Tave predictions compared to the Exponential model. Additionally, for maximum temperature (Tmax), the Spherical model also yields the best results, with RMSE = 1.497, MAE = 1.160, and MSE = 2.240, indicating its superior ability to predict Tmax. In contrast, for minimum temperature (Tmin), the Exponential model outperforms the other models, with RMSE = 1.423, MAE = 1.007, and MSE = 2.024, highlighting its greater accuracy in predicting Tmin.

Each semivariogram model demonstrates varying levels of accuracy; however, the KED estimation results using all models contribute to enhancing the accuracy of temperature estimation in East Java, as illustrated in the bar graph in Figure 8. The KED estimates, which integrate in-situ observation data and ERA5-Land data for Tave, Tmax, and Tmin, generally show improved performance with lower RMSE values. Exceptions are observed at the Nganjuk Geophysics Station and Pasuruan Geophysics Station, where the RMSE values are higher compared to the ERA5-Land temperature estimates. This discrepancy may be attributed to the notably high elevations of these stations (elevation > 700 meters above sea level, as detailed in Table 1).

Table 4. Results of Comparison of Semivariogram Model Accuracy on Daily Temporal Scale

	Metrik	***ERA5-Land***	**Exponential**	**Gaussian**	**Linear**	**Power**	**Spherical**
Tave	RMSE	1.563	1.044	1.105	1.083	1.070	**1.039**
	MAE	1.355	0.784	0.842	0.824	0.814	**0.782**
	MSE	2.444	1.090	1.220	1.172	1.145	**1.079**
Tmax	RMSE	2.805	1.488	1.484	1.553	1.551	**1.478**
	MAE	2.484	1.142	1.136	1.219	1.215	**1.134**
	MSE	7.870	2.213	2.201	2.412	2.406	**2.185**
Tmin	RMSE	1.265	**1.423**	1.528	1.456	1.472	1.448
	MAE	0.984	**1.007**	1.079	1.058	1.066	1.033
	MSE	1.600	**2.024**	2.335	2.121	2.168	2.097

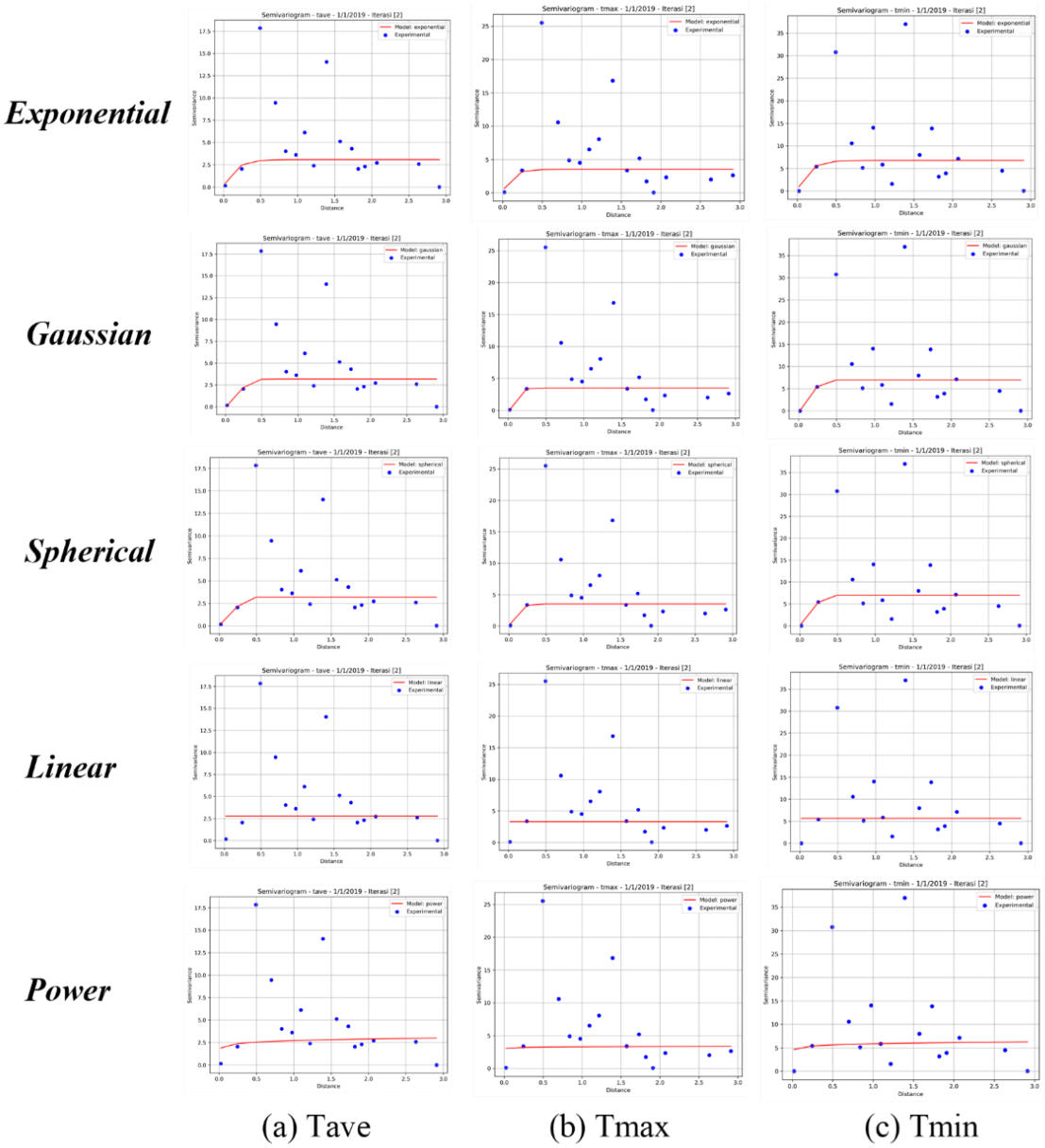

Figure 7. Example of a Semivariogram Model Graph for Estimating KED Tave, Tmax, Tmin on a Daily Scale aat Juanda Station

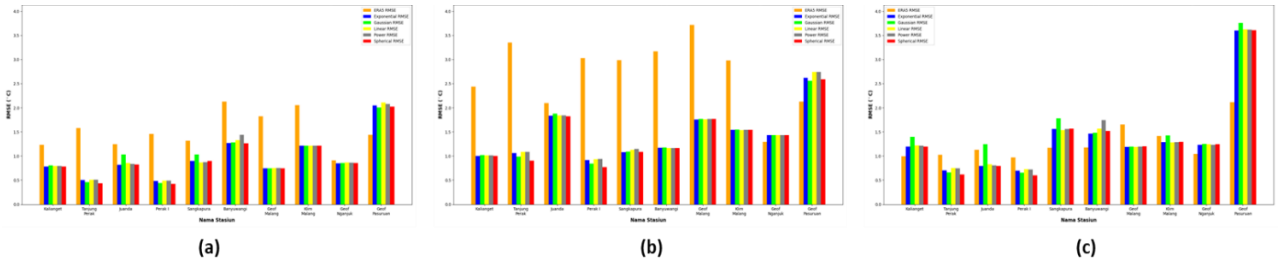

Figure 8. Graph of Daily Temporal Scale RMSE Values Before Blending Data (ERA5-Land) and After Blending (in-situ and ERA5-Land), (a) Tave, (b) Tmax, and (c) Tmin

Evaluation at the Monthly Scale

At the monthly scale, the performance of each KED semivariogram model exhibits distinct patterns, as shown in Figure 9. The Exponential, Spherical, and Gaussian models generally demonstrate similar, clear, and stable values for the sill, nugget, and range, while the Power and Linear models display irregular patterns, with unclear or absent values for these parameters. The evaluation results at the monthly scale are summarized in Table 5.

Table 5. Results of Comparison of Semivariogram Model Accuracy on a Monthly Temporal Scale

	Metrik	*ERA5-Land*	Exponential	Gaussian	Linear	Power	Spherical
Tave	**RMSE**	1.428	0.868	0.931	0.909	0.894	**0.851**
	MAE	1.293	0.637	0.712	0.663	0.658	**0.626**
	MSE	2.039	0.754	0.867	0.826	0.798	**0.724**
Tmax	**RMSE**	2.652	1.191	1.161	1.266	1.260	**1.159**
	MAE	2.425	0.927	**0.897**	1.011	1.004	0.908
	MSE	7.034	1.417	1.347	1.603	1.587	**1.344**
Tmin	**RMSE**	0.820	1.147	1.210	**1.141**	1.171	1.164
	MAE	0.647	**0.786**	0.836	0.789	0.811	0.802
	MSE	0.673	1.315	1.465	**1.302**	1.370	1.356

As indicated in Table 5, the Spherical model delivers the best performance for predicting average temperature (Tave), with RMSE = 0.851, MAE = 0.626, and MSE = 0.724, outperforming the other models. This suggests that the Spherical model is more effective in minimizing errors in Tave predictions. For maximum temperature (Tmax), the Spherical model also provides the best results, with RMSE = 1.159 and MSE = 1.344. In contrast, for minimum temperature (Tmin), the Linear model achieves the best results, with RMSE = 1.141 and MSE = 1.302, while the Exponential model yields the lowest MAE value at 0.786. The graphs for each semivariogram model are presented in Figure 9.

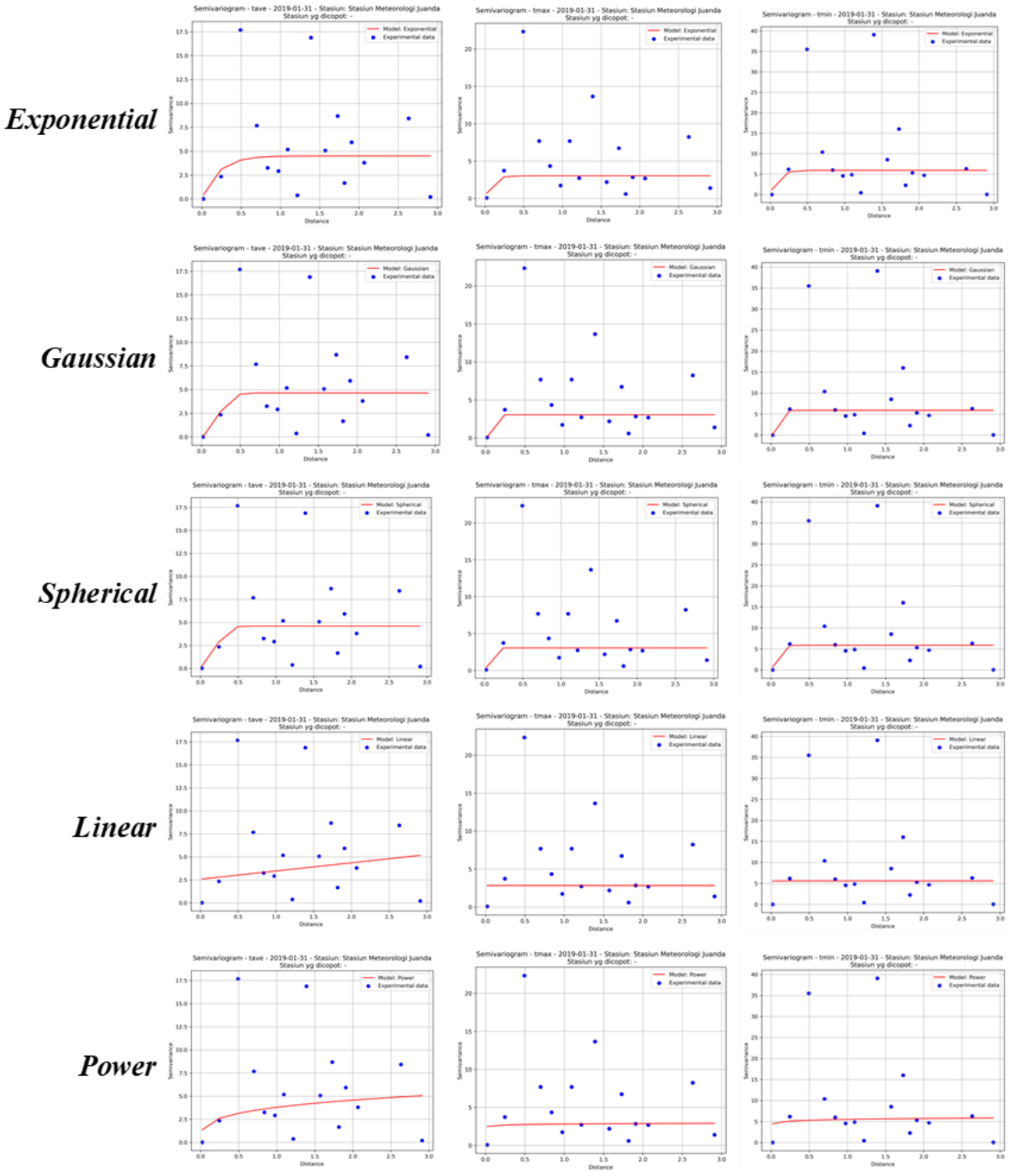

Figure 9. Semivariogram Model Graph for Monthly Scale KED Tave, Tmax, Tmin Estimation at Juanda Station

A comparison of RMSE values before and after the integration of in-situ and ERA5-Land data (shown in Figure 10) demonstrates that the combined data generally results in better performance, with lower RMSE values for Tave, Tmax, and Tmin at most study locations. However, exceptions are observed at the Pasuruan Geophysics Station for Tave, which shows an increased RMSE after data integration, and at the Sangkapura Station for Tmax, where the RMSE also increases after integration. These anomalies are likely due to the specific elevations of these stations, with Pasuruan Geophysics Station situated at an elevation of 832 meters above sea level (Table 1), and the differing distances between locations.

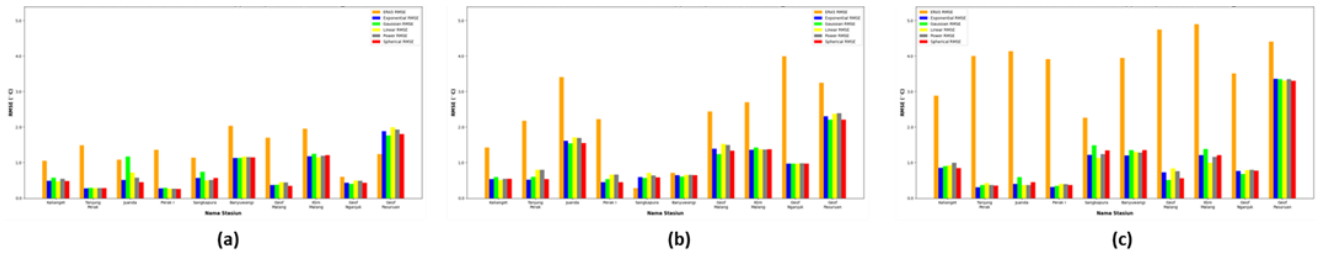

Figure 10. Graph of Monthly Temporal Scale RMSE Values before Blending Data (ERA5-Land) and After Blending (in-situ and ERA5-Land), (a) Tave, (b) Tmax, and (c) Tmin

Specifically, the results of this study highlight that the Spherical semivariogram model provides the most accurate estimates for both average temperature (Tave) and maximum temperature (Tmax). This finding aligns with the work of Sun et al. (2020), who also identified the Spherical model as the most suitable for modeling daily air temperature residuals, as it captures strong spatial correlations over short distances due to microclimate homogeneity, which then diminishes at longer distances. Additionally, the study confirms the observations of Taszarek et al. (2021), who noted the impact of elevation on accuracy, with elevation differences leading to vertical biases at each grid point that must be considered in temperature modeling.

Conclusion

The analysis and discussion presented in this study demonstrate that the Kriging with External Drift (KED) technique significantly enhances the accuracy of temperature estimations for Tmax, Tave, and Tmin. This improvement is most evident when the Spherical semivariogram model is applied. The Spherical model consistently outperforms other models, particularly in predicting Tave and Tmax, as evidenced by the lowest RMSE and MAE values. These findings indicate a superior spatial alignment between in-situ temperature data and ERA5-Land data. Additionally, the Spherical model effectively handles the large temperature fluctuations in Tmax, which is particularly prone to high variability and extreme changes. The lower RMSE suggests that the Spherical model successfully minimizes squared prediction errors, while the small MAE indicates greater consistency in predicting temperatures close to the observed values. Consequently, the Spherical model proves to be the most reliable for estimating Tave and Tmax in East Java. In contrast, for Tmin, the Exponential model yields the lowest RMSE at the daily scale, while the Linear model demonstrates superior performance at the monthly scale, with the smallest RMSE. Overall, the KED technique, particularly when combined with the Spherical model, provides more accurate temperature estimates compared to ERA5-Land data alone, especially at the monthly scale.

In light of these findings, it is recommended that further studies be conducted over a broader geographical area and with a greater number of observation sites to validate and extend the results.

Acknowledgments

The authors wish to acknowledge the Center for Human Resources Development (PPSDM) BMKG for their financial support of this research under Contract Number e.B/HM.02.03/001/KDL/I/2024. Additionally, the authors express their gratitude to BMKG and ECMWF for providing the in-situ and ERA5-Land temperature data used in this study.

References

Abbass, K., Qasim, M., Song, H., Murshed, M., Mahmood, H., & Younis, I. (2022). “A review of the global climate change impacts, adaptation, and sustainable mitigation measures”. *Environmental Science and Pollution Research International*, 29, 42539 - 42559. https://doi.org/10.1007/s11356-022-19718-6.

Ainurrohmah, S., & Sudarti, D. S. (2022). “Analisis Perubahan Iklim dan Global Warming yang Terjadi sebagai Fase Kritis”. Jurnal Pendidikan Fisika dan Fisika Terapan (Vol. 8, Issue 1).

Aldrian, E., Karmini, M., & Budiman, D. B. (2011). "Adaptasi dan mitigasi perubahan iklim di Indonesia". Pusat Perubahan Iklim dan Kualitas Udara, Kedeputian Bidang Klimatologi, Badan Meteorologi, Klimatologi, dan Geofisika.

Alfiandy, S., Rangga, I. A., & Permana, D. S. (2022). "Pola Peningkatan Suhu Udara Berdasarkan Data Bmkg Dan Era5 Di Provinsi Sulawesi Tengah". Jurnal Analisis Kebijakan Kehutanan, 19(1), 63–70. https://doi.org/10.20886/jakk.2022.19.1.63-70

Benjamin Murphy, Roman Yurchak, & Sebastian Müller. (2024). GeoStat-Framework/PyKrige: v1.7.2 (v1.7.2). Zenodo. https://doi.org/10.5281/zenodo.11360184

Berrar, D. (2019). Cross-validation.

Bohling, G. (2005). "Introduction to geostatistics and variogram analysis". *Kansas geological survey*, *1*(10), 1-20.

Cao, B., Gruber, S., Zheng, D., & Li, X. (2020). "The *ERA5-Land* soil temperature bias in permafrost regions. Cryosphere", 14(8), 2581–2595. https://doi.org/10.5194/tc-14-2581-2020

Carleton, T., & Hsiang, S. (2016). "Social and economic impacts of climate". *Science*, 353. https://doi.org/10.1126/science.aad9837.

Chen, L., Wang, X., Cai, X., Yang, C., & Lu, X. (2021). "Seasonal Variations of Daytime Land Surface Temperature and Their Underlying Drivers over Wuhan, China". *Remote. Sens.*, 13, 323. https://doi.org/10.3390/rs13020323.

Chen L, Gao Y, Zhu D, Yuan Y, Liu Y (2019). "Quantifying the scale effect in geospatial big data using semi-variograms". PLOS ONE 14(11): e0225139. https://doi.org/10.1371/journal.pone.0225139

Choudhury, D., Ji, F., Nishant, N., & Di Virgilio, G. (2023). "Evaluation of ERA5-Simulated Temperature and Its Extremes for Australia". Atmosphere, 14(6). https://doi.org/10.3390/atmos14060913

Copernicus Climate Change Service, *ERA5-Land* Hourly Data From 1950 to Present Available online (2022) https://cds.climate.copernicus.eu/doi/10.24381/cds.e2161bac

Cressie, N. (2015). Statistics for spatial data. John Wiley & Sons.

Camana, F., & Deutsch, C. (2020). The Nugget Effect. .

Duan, S. B., Li, Z. L., Li, H., Göttsche, F. M., Wu, H., Zhao, W., Leng, P., Zhang, X., & Coll, C. (2019). "Validation of Collection 6 MODIS land surface temperature product using *in-situ* measurements". Remote Sensing of Environment, 225, 16–29. https://doi.org/10.1016/j.rse.2019.02.020

Dunn, R. J. H., Alexander, L. V., Donat, M. G., Zhang, X., Bador, M., Herold, N., Lippmann, T., Allan, R., Aguilar, E., Barry, A. A., Brunet, M., Caesar, J., Chagnaud, G., Cheng, V., Cinco, T., Durre, I., de Guzman, R., Htay, T. M., Wan Ibadullah, W. M., … Bin Hj Yussof, M. N. A. (2020). "Development of an Updated Global Land *In-situ*-Based Data Set of Temperature and Precipitation Extremes: HadEX3". Journal of Geophysical Research: Atmospheres, 125(16).https://doi.org/10.1029/2019JD032263

Goovaerts, P. (1997). Geostatistics for natural resources evaluation. Oxford university press.

Gregg, W. W., & Conkright, M. E. (2001). Global seasonal climatologies of ocean chlorophyll: "Blending *in-situ* and satellite data for the Coastal Zone Color Scanner era". Journal of Geophysical Research: Oceans, 106(C2), 2499–2515. https://doi.org/10.1029/1999jc000028

Haberlandt, U. (2007). "Geostatistical interpolation of hourly precipitation from rain gauges and radar for a large-scale extreme rainfall event". *Journal of Hydrology*, 332, 144-157. https://doi.org/10.1016/J.JHYDROL.2006.06.028.

Hersbach, H., Bell, B., Berrisford, P., Hirahara, S., Horányi, A., Muñoz-Sabater, J., ... & Thépaut, J. N. (2020). "The ERA5 global reanalysis. *Quarterly journal of the royal meteorological society"*, *146*(730), 1999-2049.

Hendarwati, E. K., Lepong, P., & Suyitno, S. (2023). "Pemilihan *Semivariogram* Terbaik Berdasarkan Root Mean Square Error (RMSE) pada Data Spasial Eksplorasi Emas Awak Mas". GEOSAINS KUTAI BASIN, 6(1), 47-52.

Hidayati, I. N., & Suryanto, S. (2015). "Pengaruh perubahan iklim terhadap produksi pertanian dan strategi adaptasi pada lahan rawan kekeringan". *Jurnal Ekonomi & Studi Pembangunan*, 42-52.

Hodson, T. O. (2022). "Root mean square error (RMSE) or mean absolute error (MAE): When to use them or not. Geoscientific Model Development Discussions", 2022, 1-10. https://doi.org/10.5194/gmd-15-5481-2022

Huang, X., Han, S., & Shi, C. (2022). "Evaluation of Three Air Temperature Reanalysis Datasets in the Alpine Region of the Qinghai–Tibet Plateau". Remote Sensing, 14(18). https://doi.org/10.3390/rs14184447

Hudson, G., & Wackernagel, H. (1994). "Mapping temperature using kriging with external *drift*: Theory and an example from scotland". *International Journal of Climatology*, 14, 77-91. https://doi.org/10.1002/JOC.3370140107.

Jurusan, P., Pertambangan, T., Teknik, A., Nasional, P., & Ringkasan, B. (2018). "Efektivitas Ordinary Cokriging Dan Kriging Untuk Karakterisasi Potensi Manifestasi Panas Bumi Ishaq". In Print) Jurnal INTEKNA (Vol. 18, Issue 2). Online. http://ejurnal.poliban.ac.id/index.php/intekna/issue/archive

Ly, S., Charles, C., & Dégre, A. (2011). "Geostatistical interpolation of daily rainfall at catchment scale: the use of several variogram models in the Ourthe and Ambleve catchments, Belgium". *Hydrology and Earth System Sciences*, 15, 2259-2274. https://doi.org/10.5194/HESS-15-2259-2011.

Lobell, D. B., Roberts, M. J., Schlenker, W., Braun, N., Little, B. B., Rejesus, R. M., & Hammer, G. L. (2014). "Greater sensitivity to drought accompanies maize yield increase in the U.S. Midwest". Science, 344(6183), 516–519. https://doi.org/10.1126/science.1251423

Laporan IPCC, (2021) https://unfccc.int/topics/science/workstreams/cooperation-with-the-ipcc/the-sixth-assessment-report-of-the-ipcc

Muñoz-Sabater, J., Dutra, E., Agustí-Panareda, A., Albergel, C., Arduini, G., Balsamo, G., Boussetta, S., Choulga, M., Harrigan, S., Hersbach, H., Martens, B., Miralles, D. G., Piles, M., Rodríguez-Fernández, N. J., Zsoter, E., Buontempo, C., & Thépaut, J. N. (2021). "*ERA5-Land*: A state-of-the-art global reanalysis dataset for land applications". Earth System Science Data, 13(9), 4349–4383. https://doi.org/10.5194/essd-13-4349-2021

Mazzella, A., & Mazzella, A. (2013). "The importance of the model choice for experimental *semivariogram* modeling and its consequence in evaluation process". Journal of Engineering, 2013(1), 960105. https://doi.org/10.1155/2013/960105

Oliver, M., & Webster, R. (2014). "A tutorial guide to geostatistics: Computing and modelling variograms and kriging". *Catena*, 113, 56-69. https://doi.org/10.1016/J.CATENA.2013.09.006

Oliver, M. A., & Webster, R. (2015). "Basic steps in geostatistics: the variogram and kriging" (Vol. 106). Cham, Switzerland: Springer International Publishing.

Pawitan, H., & Sophaheluwakan, A. (n.d.)." Validasi Dan Koreksi Data Satelit Trmm Pada Tiga Pola Hujan Di Indonesia Validation And Correction Of Trmm Satellite Data On Three Rainfall Patterns In Indonesia.

Prasetyo, S., Hidayat, U., Haryanto, Y. D., & Riama, N. F. (2021). "Variasi dan Trend Suhu Udara Permukaan di Pulau Jawa Tahun 1990-2019". Jurnal Geografi : Media Informasi Pengembangan Dan Profesi Kegeografian, 18(1), 60–68. https://doi.org/10.15294/jg.v18i1.27622

Rozalia, G., Yasin, H., & Ispriyanti, D. (2016). "Penerapan Metode Ordinary Kriging Pada Pendugaan Kadar No 2 Di Udara (Studi Kasus: Pencemaran Udara di Kota Semarang)". JURNAL GAUSSIAN, 5(1), 113–121. http://ejournal-s1.undip.ac.id/index.php/gaussian

Shamshiri, R. R., Jones, J. W., Thorp, K. R., Ahmad, D., Man, H. C., & Taheri, S. (2018). "Review of optimum temperature, humidity, and vapour pressure deficit for microclimate evaluation and control in greenhouse cultivation of tomato: a review". In International Agrophysics (Vol. 32, Issue 2, pp. 287–302). Walter de Gruyter GmbH. https://doi.org/10.1515/intag-2017-0005

Varentsov, M., Esau, I., & Wolf, T. (2020). "High-Resolution Temperature Mapping by Geostatistical Kriging with External *Drift* from Large-Eddy Simulations". *Monthly Weather Review*. https://doi.org/10.1175/mwr-d-19-0196.1.

Velasco-Forero, C. A., Sempere-Torres, D., Cassiraga, E. F., & Jaime Gómez-Hernández, J. (2009). "A non-parametric automatic blending methodology to estimate rainfall fields from rain gauge and radar data". Advances in Water Resources, 32(7), 986–1002. https://doi.org/10.1016/j.advwatres.2008.10.004

Tang, W., Zhang, L., & Banerjee, S. (2021). "On identifiability and consistency of the nugget in Gaussian spatial process models". *Journal of the Royal Statistical Society Series B: Statistical Methodology*, *83*(5), 1044-1070.

Yang, W., Wang, Y., Webb, A., Li, Z., Tian, X., Han, Z., Wang, S., & Yu, P. (2018). "Influence of climatic and geographic factors on the spatial distribution of Qinghai spruce forests in the dryland Qilian Mountains of Northwest China". *The Science of the total environment*, 612, 1007-1017 . https://doi.org/10.1016/j.scitotenv.2017.08.180.

Zhao, P., & He, Z. (2022). “A First Evaluation of *ERA5-Land* Reanalysis Temperature Product Over the Chinese Qilian Mountains”. Frontiers in Earth Science, 10. https://doi.org/10.3389/feart.2022.907730

Zhao, Q., Guo, Y., Ye, T., Gasparrini, A., Tong, S., Overcenco, A., Urban, A., Schneider, A., Entezari, A., Vicedo-Cabrera, A. M., Zanobetti, A., Analitis, A., Zeka, A., Tobias, A., Nunes, B., Alahmad, B., Armstrong, B., Forsberg, B., Pan, S. C., … Li, S. (2021). “Global, regional, and national burden of mortality associated with non-optimal ambient temperatures from 2000 to 2019: a three-stage modelling study”. The Lancet Planetary Health, 5(7), e415–e425. https://doi.org/10.1016/S2542-5196(21)00081-4

Zhou, X., Okaze, T., Ren, C., Cai, M., Ishida, Y., Watanabe, H., & Mochida, A. (2020).” Evaluation of urban heat islands using local climate zones and the influence of sea-land breeze”. *Sustainable Cities and Society*, 55, 102060. https://doi.org/10.1016/j.scs.2020.102060.